ASPS Conference Proceedings 1: 1149-1157 (2022)

Proceedings of

12th Structural Engineering Convention-An International Event (SEC 2022)

Available at https://asps-journals.com/index.php/acp

Optimal control of structural vibration using LQG algorithm

Payel Chaudhuri [1, *], D.K. Maiti [2], Damodar Maity [1]

[1] Civil Engineering Department, Indian Institute of Technology, Kharagapur -721302, India.
[2] Aerospace Engineering Department, Indian Institute of Technology, Kharagapur -721302, India.

Paper ID - 070534

Abstract

This paper proposes a Linear Quadratic Guassian Design (LQG) with based semi-active control algorithm for vibration reduction of building structures. The controlled damper force required by the structure has been calculated from an MR damper of load capacity 100N. A building frame has been selected to illustrate the performance of the proposed algorithm. Four different earthquake acceleration data has been used as input vibration data to the numerical frame. The proposed method of damping on the frame has been found to be more effective to reduce the structural response significantly in comparison with the conventional tuned liquid column damper. The developed method is efficient in providing the optimum control force required to the frame. Therefore, it minimizes the need of high damping capacity and the number of dampers. As a result, it reduces the cost of maintenance and structural control during earthquakes.

Keywords: Semi-active control, Magneto rheological damper, clipped optimal control, Linear Quadratic Gaussian, tuned liquid column damper

1. Introduction

Different control systems and dampers have been studied to reduce the effect of seismic hazards in structures by researchers. Structural control is the one of the most effective way to achieve this goal. Semi-active control is found to be more effective than passive and active system.[1, 2] Effective performance of the damping devices has become very important to ensure structural safety and serviceability criteria. Magneto rheological (MR) damper [3,4,5] appears to be promising for seismic protection of structures. It has advantages such as very low power consumption; ability to provide a readily controllable damping force, large achievable force capacity, low sensitivity to temperature changes and different control algorithms can be used for optimum performance. A magneto rheological damper [6] is filled with magneto rheological fluid which is controlled by magnetic field generated by passing electric current. When MR fluid is exposed to a magnetic field, dispersed micron-size iron particles align themselves along magnetic flux lines throughout the fluid.[7] The iron particles resist being moved out of their respective flux lines and act as a barrier to fluid flow. The fluid viscosity increases within the damper as the current intensity increases and therefore the resistance to flow.

Throughout the years, different researchers have tried to perform the vibration control of building structures by installing MR damper combining with various control algorithms[8, 9] conducted a comparative study of different algorithms i.e., lyapunov stability theory, decentralized bang bang control, clipped optimal control, decentralized output feedback polynomial controller, simple passive control algorithms to evaluate control force and required voltage for the MR dampers. Kwok et al.[10] developed multi objective binary coded GA to compare with passive control. Uz[11] performed a coupled building control where two adjacent shear buildings were considered with semi-active dampers installed in between those buildings. Aly[12] developed control algorithms[37,38,39,40] which were inspired by different other existing algorithms. The variation of input voltage of MR damper with respect to time was also considered. Kim[13] studied the effectiveness of smart top story isolation method for vibration control of the structures during seismic effect of a 20 DOFs shear building with MR damper. Chang et al.[14] installed MR dampers in outrigger system to their building model. MR dampers were located between the outriggers and the perimeter columns. Bathaei et al.[15] have implemented both tuned mass damper and MR damper together on a 11 degree of freedom building model as semi-active control using two types

*Corresponding author. Tel: +91 3222 255 221; E-mail address: payelce@gmail.com

Published online: December 19, 2022
doi:10.38208/acp.v1.634

of Fuzzy controllers. Hu et al.[16] used clipped optimal control based on linear quadratic regulator algorithm to evaluate MR damper control forces. Gendeshmin et al.[17] have done numerical simulation of an MR damper attached building frame using block pulse function as control algorithm.

It can be observed from the aforementioned literature that the researchers have studied mainly on the following points.

- Until now, the parameters of damping devices were the main area of focus in the field of structural control in civil engineering.
- The behavior of the building frame has not been stabilized and controlled by proper control theory.
- A linear optimal controller has been attached with the damper to generate the required control force to the structure.

The present study proposes a semi-active control combining LQG control with clipped optimal control. LQG controller is unique and is simply a combination of Kalman filter i.e., a linear quadratic estimator (LQE) and linear quadratic regulator (LQR). Both the filters can be designed independently. LQG control applies to both linear time varying systems and linear time invariant systems. LQG Controller operates on a linear dynamic feedback law and works as a dynamic system like the system it controls. LQG Controller and the system both have the same state dimension. Therefore, this controller can be easily implemented and computed numerically in comparison with conventional control algorithms i.e., clipped optimal control. Clipped optimal controller has been popular to compute the voltage required to the damper to generate control force. The voltage required by MR damper to generate the required damper force is calculated by Clipped optimal control method.

A linear MR damper[18] designed based on Bingham model and is installed to a three storey frame to reduction the vibration effect on the frame. MR damper location was optimized. The efficiency of MR damper over a TLCD controlled building frame was evaluated. Efficacy of the proposed algorithm has been evaluated in comparison with the conventional LQG controlled MR damper-building frame system. Parametric study has been carried out for four different earthquakes in two different Building frame models.

2. Semi-active control of frame

One symmetric was modeled and dynamic and state space modeling of the frame was performed. An MR damper of 100N load capacity is introduced to model Linear Quadratic Gaussian (LQG) control designed The LQG algorithm optimize the damper force generate from the MR damper according to the need of the vibrated structural frame for different seismic excitations. Therefore, the optimized MR damper force reduces the vibration of structural frames up to optimal level. A comparison of the proposed semi-active method is performed with that of a TLCD installed structural frame case. The equation of motion[19, 41] of the frame with structural Rayleigh damping for the nodal displacements u is given in Equation 1.

$$M\ddot{u} + C\dot{u} + Ku = f_g(t) \tag{1}$$

Where, M is the mass matrix, C is the damping matrix as given in Equation 2, K is the stiffness matrix, u is the displacement response due to $f_g(t)$ dynamic load with time t. Rayleigh damping is used with damping ratio 1% -2% for high rise building.

$$C = a_0 M + a_1 K \tag{2}$$

where, a_0 and a_1 have units of s^{-1} and s, respectively. The damping ratio in n^{th} mode is calculated as per the following Equation 3.[19]

$$\xi_n = \frac{a_0}{2}\frac{1}{\omega_n} + \frac{a_1}{2}\omega_n \tag{3}$$

where, ω_n is the natural frequency of n^{th} mode. Equation (1) can be further modified to Equation (4) to show the contribution of two dynamic input forces to the structural frame such as earthquake vibration force and feedback-controlled MR damper force.

$$M\ddot{u} + C\dot{u} + Ku = \Gamma f - M\Lambda\ddot{x}_g \tag{4}$$

$$\Gamma = [1 \quad 0 \quad 0]^T;\ \Lambda = [1 \quad 1 \quad 1]^T \tag{5}$$

The state space model of a dynamic system[20] described in Equation (1) and Equation (4) can be represented with state space equation and output equation as shown in Equation (6) and Equation (7) respectively.

$$\dot{z} = Az + Bf + G\ddot{x}_g \tag{6}$$

$$y = Cz + Df + v_m \tag{7}$$

The vectors z and x in this model can be represented as Equation (8).

$$z = \begin{bmatrix}\dot{u}\\ u\end{bmatrix};\ \mathrm{x} = \begin{bmatrix} f \\ \ddot{x}_g\end{bmatrix} \tag{8}$$

f is the measured force generated between the structural frame and MR damper. v_m is the measurement noise vector. The state space model has been prepared according to the Equation (6) and Equation (7) are shown in Equation (9).

$$A = \begin{bmatrix} -M^{-1}C & -M^{-1}K \\ 0 & \Lambda \end{bmatrix}; B = \begin{bmatrix} -M^{-1}\Gamma & -\Gamma \\ 0 & -\Lambda \end{bmatrix}; C = \begin{bmatrix} -M^{-1}K & -M^{-1}C \\ \Gamma & 0 \end{bmatrix}; D = \begin{bmatrix} -M^{-1}\Gamma \\ 0 \end{bmatrix} G = -\begin{bmatrix} 0 \\ \Lambda \end{bmatrix} \tag{9}$$

Here, the displacement response of the frame has been calculated through linear simulation of the dynamic system. Controllability[21] property plays a crucial role in many control structural frames, for stabilization of unstable systems by feedback, or optimal control.

3. Linear MR damper

A model of three storey frame is considered with a single MR damper to develop a suitable method to control the responses. In this model, in the post-yield area (for a stress greater than the shear stress, which depends on the magnetic field strain H, i.e. for $(\tau \geq \tau_y)$,the MR fluid behaves like a visco-plastic material. For positive values of the shear rate, $\dot{\gamma}$, the total stress is given in Equation (10).

$$\tau = \tau_{y(field)} + \mu\dot{\gamma} \tag{10}$$

Where, $\tau_{y(field)}$ is the yield stress induced by the magnetic (or electric) field and μ is the viscosity of the fluid. The Bingham model [26] consists of a Coulomb friction element placed in parallel with a viscous damper. In this model, for nonzero piston velocities, the force generated by the device is given in Equation (11).

$$F = f_c sgn(\dot{x}) + c_0 x + f_0 \tag{11}$$

Where, c_0 is the damping coefficient and f_c is the frictional force, which is related to the fluid yield stress and f_0 is the accumulator force generated due to piston movement. An offset in the force is included to account for the nonzero mean observed in the measured force due to the presence of the accumulator. The parameters considered for modeling the MR damper numerically are $f_c = 95\text{N}$, $c_0 = 50\text{N}.\frac{\text{sec}}{\text{cm}}$, $f_0 = -10N$. The command voltage has a maximum value of 10v. The linear MR damper force is modeled in MATLAB programming. The initial damper force generated considering the parameters are shown in Fig. 1. The damping force generated from the linear model is further optimized by the developed algorithm (LQG) as per the requirement of the vibration structural frame in the study.

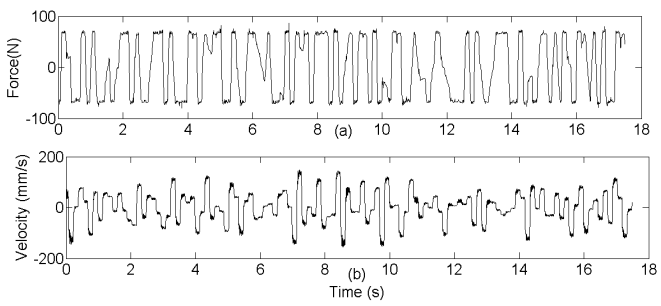

Fig. 1 Force of a linear MR damper

Fig.2 Linear time –invariant system

4. Linear Quadratic Gaussian (LQG) controller

Optimal control design is based on obtaining a system that is the best possible with respect to a certain performance index or design criterion.[20] An optimal control structural frame uses the state space representation of the system as in equations Equation (6) and Equation (7) and it can be mathematically represented by the following Equation (12). A linear time invariant system is shown in Fig. 2.

$$J = \int_{t_1}^{t_2} F[z(t), x(t), t]dt \tag{12}$$

Equation (12) is subjected to the constraint described in Equation (6). The initial state is considered as $z(t_1) = z_0$. The performance index J is a scalar quantity and consists of the integral of scalar function of state vector and control vector. The state equation of the dynamic system in Equation (6) which is to be controlled is interpreted as constraints in this control design problem. In a linear system, the design objective is to keep the states of the system at an equilibrium state and the system should be able to return to its equilibrium state from any initial state. Therefore, the performance index of a Linear Quadratic Gaussian problem can be written by means of a linear regulator problem. The objective is to find the control input force f which at every time t only depends upon the past output $y(t_1), 0 \leq t_1 < t$ such that the following quadratic cost function in Equation (13) is minimized for $F \geq 0; Q(t) \geq 0; R(t) \geq 0;$

$$J = E_d[z^T(t_1)F(t_1)z(t_1) + \int_{t_2}^{t_1} (z^T Q z + x^T R x)dt$$

where, the constraints are placed on both the state and control vectors. E_d denotes the expected value. The final time (horizon) T may be either finite or infinite. If the horizon tends to infinity the first term $z^T(t_1)F(t_1)z(t_1)$ of the cost function becomes negligible and irrelevant to the problem. The LQG controller solves the LQG control problem specified by a set of equations in Equation (14).

$$\begin{aligned}\dot{\hat{z}}(t) = A(t)\hat{z}(t) + B(t)x(t) \\ + K_a(t)\big(y(t) - C(t)\hat{z}(t)\big), \hat{z}(0) \\ = E_d[z(0)]\end{aligned}$$

$$x(t) = -L_a(t)\, \hat{z}(t) \tag{14}$$

Kalman gain and feedback gain are shown in the following Equation (15) and Equation (16).

$$K_a(T) = P(t)C^T(t)W^{-1}(t) \quad (15)$$

$$L_a(t) = R^{-1}(t)B^T(t)S(t) \quad (16)$$

$K_a(t)$ can be computed by solving the following Ricatti equation in Equation (20) that solves Linear quadratic estimation problem (LQE).

$$\dot{P}(t) = A(t)P(t) + P(t)A^T(t) - P(t)C^T(t)W^{-1}(t)C(t)P(t) + V_m(t)$$

$$P(0) = E_d[(z(0)z^T(0))] \quad (17)$$

$L_a(t)$ can be calculated similarly by solving the following Ricatti equation in Equation (18) that solves Linear quadratic regulator problem (LQR).

$$-\dot{S}(t) = A^T(t)S(t) + S(t)A(t) - S(t)B(t)R^{-1}(t)B^T(t)S(t) + Q(t)$$

$$S(T) = F \quad (18)$$

Given the solution $P(t), 0 \le t \le T$ and $S(t), 0 \le t \le T$. The controller $K_c(s)$ has been developed using LQG methods[8] which was defined previously. The major advantage of the LQG design is that it not only controls the output response of the controllable states for desired values but also reduce the response of uncontrollable states. A structural frame control with MR damper on top floor is depicted in Fig. 3.

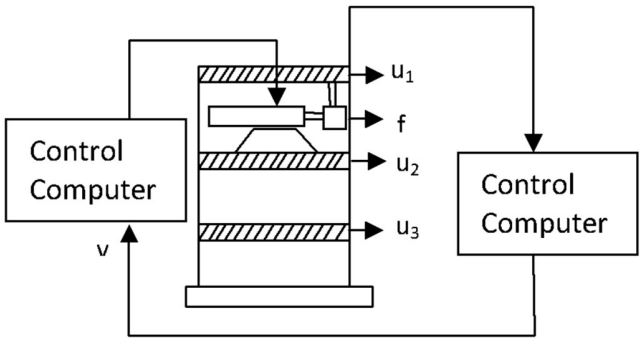

Fig. 3 A three story structural frame control system with MR damper on top floor

5. Clipped optimal controller

The control force and the voltage required for the MR damper to generate the optimal LQG controlled damping force is calculated and controlled using a clipped-optimal controller throughout the simulation. The control force, F_o based on the measured responses y, and the measured force F_m from the Equation (19).

$$F_o = L^{-1}\left[K_c(s)L\begin{bmatrix} y \\ F_m \end{bmatrix}\right] \quad (19)$$

Where, L is a Laplace Transform. The compensator gain has been obtained from LQG strategy. The force generated by the MR damper cannot be changed directly only the voltage applied to the current driver for the MR damper can be directly changed. The algorithm for selecting the command signal is graphically represented in Fig. 3 and can be concisely stated in Equation (20).

$$v = V_{max}H\{(F_o - F_m)F_m\} \quad (20)$$

Where, V_{max} is the voltage to the current driver associated with saturation of the magnetic field in the MR damper and H is the Heaviside step function and v is the voltage required.

6. Tuned Liquid Column (TLCD) Damping

To evaluate the ability of MR damper over passive dampers, a passive tuned liquid column damper has been developed and a comparative study is done in the present work. Tuned liquid column damper[27] is generally used as a passive damper for vibration reduction for many years. Compared to other passive dampers, the advantages of TLCDs comprise low installation costs, easy application to either new buildings or retrofitting existing structural frames, a simple tuning mechanism and virtually no maintenance requirements. In the present study, a tuned liquid column damper has been designed numerically and attached to the top floor[28,29,30] of the aforementioned structural frame. A model of a structural frame with a TLCD is shown in Fig. 4.

The dynamic equation of the structural frame (Equation 1) attached with TLCD and the TLCD alone was represented in Equation (21 to 24).

Primary mass:

$$(M + m_d)\ddot{u} + C\dot{u} + Ku = -M\Lambda\ddot{x}_g - m_d \quad (21)$$

$$\Lambda = [1 \quad 1 \quad 1]^T$$

Damper:

$$m_d\ddot{u_d} + c_d\dot{u_d} + k_du_d = -m_d\ddot{u} \quad (22)$$

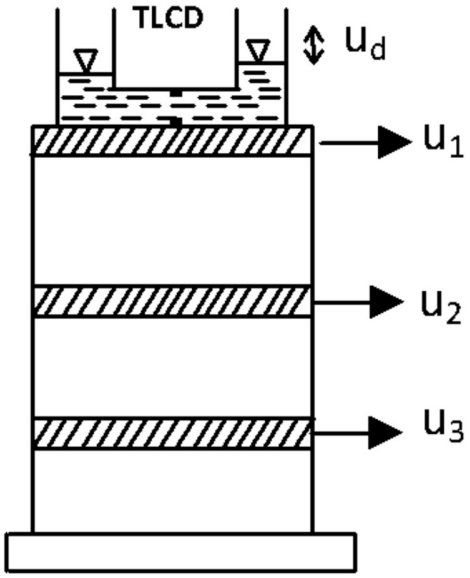

Fig. 4 A three story structural frame control system with TLCD on top floor

Both the equations are combined to form the following equation of motion of the structural frame with TLCD shown in Equation (26) –Equation (27).

$$M'\ddot{U} + C\dot{U} + KU = -M^*\Lambda\ddot{x}_g \tag{23}$$

where the matrices are defined as:

$$M' = \begin{bmatrix} M + m_d & m_d Bi/Li \\ m_d Bi/Li & m_d \end{bmatrix}; K = \begin{bmatrix} K & 0 \\ 0 & k_d \end{bmatrix}; C = \begin{bmatrix} C & 0 \\ 0 & c_d \end{bmatrix}; M^* = \begin{bmatrix} M + m_d \\ m_d Bi/L i \end{bmatrix}; \tag{24}$$

The parameters[31] considered to model the numerical TLCD are given in Table 1.

A state space representation for TLCD-structural frame dynamic model (Equation 21 to 24) has been developed simultaneously. The vibration response of this combined model of the structural frame taken in the paper was calculated through linear simulation. They are compared with that of the proposed MR damper controlled structural frame for the efficiency of the later.

1. Three Storey frame

A structural frame is considered to demonstrate the efficiency of the developed algorithm using four different earthquake data. One three story structural frame has been adopted from Dyke et al.[34] and is shown in a Fig. 5. The system matrices of the frame are shown in the table (Table 2).

Table 1 Parameters for TLCD used in the study

ms	normalized mass of the structural frame considered
mu (mass ratio)	0.002 (assumed)
m_d (total mass of liquid)	mu ∗ ms
den (density of liquid)	1000
fr (frequency ratio)	(sqrt(1 − (mu/2)))/(1 + mu) = 0.984[32]
w0 (frequency of structural frame)	First natural frequency of the structural frame
g	9.81
aa	Maximum absolute acceleration
del (head loss coefficient)	3.58 ∗ mu/(aa/g) = 0.7
Li (Total length of the liquid)	(2 ∗ g)/(fr ∗ fr ∗ w0 ∗ w0)[33]
Alpha (liquid length ratio)	0.8(assumed)
Ai (area of the TLCD)	mu ∗ ms/(den ∗ Li) [33]
m_dBi/Li (mass of liquid in horizontal direction)	den ∗ Ai ∗ Bi
Bi (horizontal length of liquid)	Alpha ∗ L
stdev (standard deviation of liquid velocity)	0.1 (calculated through trial and error method)
k_d (stiffness of TLCD)	2 ∗ density ∗ Ai ∗ g [30]
c_d (damping coefficient)	density ∗ Ai ∗ del ∗ stdev/sqrt(2 ∗ 3.141)[33]

Table 2 System Matrices of Structural frame

	Values
Mass Matrix, [M]	$M = \begin{bmatrix} 98.3 & 0 & 0 \\ 0 & 98.3 & 0 \\ 0 & 0 & 98.3 \end{bmatrix}$ kg
Stiffness Matrix,[K]	$K = \begin{bmatrix} 12 & -6.84 & 0 \\ -6.84 & 13.7 & -6.84 \\ 0 & -6.84 & 6.84 \end{bmatrix} 10^5 \frac{N}{m}$
Damping Matrix, [C]	$C = \begin{bmatrix} 175 & -50 & 0 \\ -50 & 100 & -50 \\ 0 & -50 & 50 \end{bmatrix} \frac{Ns}{m}$
Location Matrix of MR Damper force	$\Gamma = [1 \quad 0 \quad 0]^T$
External force distribution matrix	$\Lambda = [1 \quad 1 \quad 1]^T$

2. RESULTS AND DISCUSSION

Four recorded earthquake data (Fig. 5) are considered to excite the structural frame. These data are NS component of El-Centro (South California, USA) earthquake acceleration data (1940), Lomapreita earthquake (North California, USA) acceleration data (October, 1989), EW component of Arizona earthquake acceleration data (June, 2008), and EW component of Fukushima earthquake acceleration data (November, 2011) respectively.

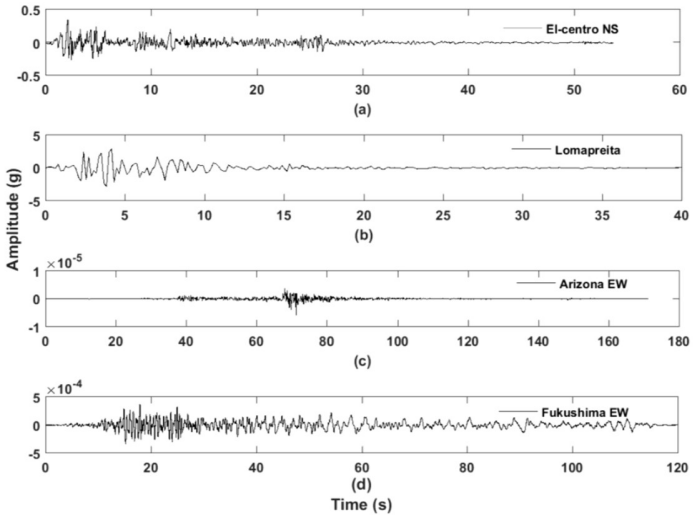

Fig. 5 Different types of earthquake acceleration data

3. LQG controlled MR damper

In this section, the efficacy of the proposed method i.e., LQG controlled MR damper on the response of the structural frame have been assessed against an uncontrolled frame and TLCD placed on top of frame.

Top floor responses for all the above cases were obtained in terms of time domain responses (acceleration (Fig. 6) and displacement (Fig. 7) response of the structural frame) and frequency domain responses i.e., frequenc response function (FFT) (Fig. 8) and power spectral density (PSD) (Fig. 9)) of displacement response). Table 3 - 4 shows the maximum displacement and RMS value of PSD curve for displacement in top floor for all the above mentioned models using four different earthquake data.

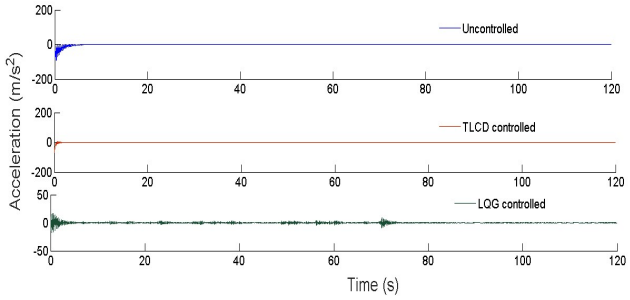

Fig. 6 Acceleration for Fukushima EW component of earthquake

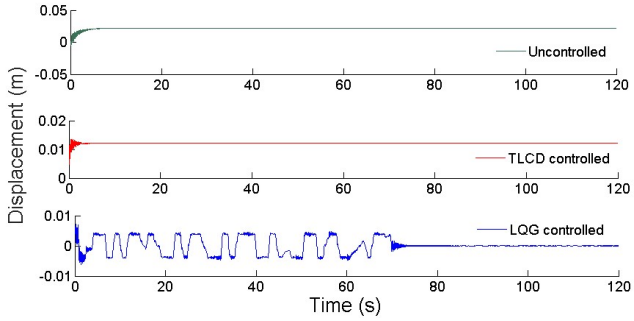

Fig. 7 Displacements for Fukushima EW component of earthquake

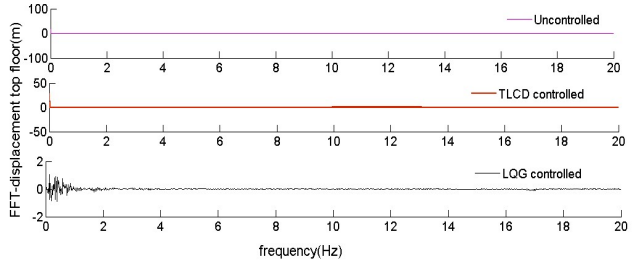

Fig. 8 FFT for Fukushima component of earthquake

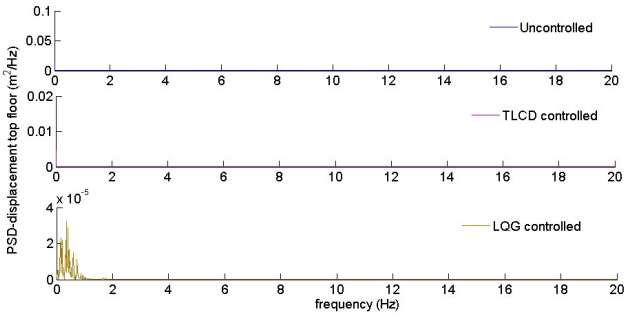

Fig. 9 PSD curve for Fukushima component of earthquake

Table 4 RMS of PSD (displacement) curve in top floor (mm)

Earthquakes	Uncontrolled structural frame	TLCD controlled	LQG controlled
El Centro NS	10.7	6.0	1.2
Lomapreita	10.5	6.0	1.2
Arizona EW	10.9	6.0	1.2
Fukushima	10.8	6.0	1.2

Table 3 Maximum displacement in top floor (mm)

Earthquakes	Uncontrolled structural frame	TLCD controlled	LQG controlled
El Centro NS	21.98	13.5	7.5
Lomapreita	22	14.6	6.8
Arizona EW	21.9	13.4	7.2
Fukushima	22	13.5	7.2

It is observed from Table 3-4 that for Fukushima EW data, TLCD and LQG controlled MR damper have reduced the uncontrolled maximum amplitude of displacement up to 62% and 32% whereas RMS displacements are reduced up to 55% and 11% respectively. Similarly, when LQG-PSO controlled MR damper has been used, the maximum amplitude of displacement and RMS displacements have reduced up to 17% and 4.6% of uncontrolled maximum amplitude of displacement and RMS displacement respective. It can be finally concluded that the proposed LQG-PSO controlled MR damper is more effective in reducing the earthquake induced displacement compared to conventional LQG controlled MR damper and conventional TLCD.

LQG based MR damper-structural frame have reduced the responses of the structural frame significantly compared to a TLCD–structural frame model. The simulation results of confirms that the combined LQG control algorithm has performed effectively better in reducing the structural response to a greater extent in TLCD controlled structural frame. Therefore, it can be concluded that the developed methodology is effective enough to reduce the responses in different loading condition of structural frame.

4. CONCLUSION

The study consists of proposing a method i.e., a combined Linear Quadratic Gaussian Design with clipped optimal control based semi-active control algorithm for vibration reduction of structural frame. LQG is a control method for semi-active control systems and is compatible with MR dampers. A clipped optimal controller has been used to minimize the voltage required by MR damper to produce damper force. The method shows much flexibility to produce desirable range of outputs in different loading conditions. A linear MR damper is modeled to produce the controller optimal force to the frame. The performance of an efficient controller can control the vibration of structures significantly. The location optimization of MR damper reveals that the MR damper is found to perform best when it is placed on top floor of the structural frame. The study reveal that the proposed semi-active control method is efficient in reducing the undesirable displacement of the structural frame due to different types of earthquake data. The method can also reduce the necessity to optimize the parameters of MR damper for required optimum damper force. An experimental study of parameters of MR dampers can also be done to evaluate the level of MR damper performance along with the controller requirement. The proposed method of controlling the structure itself can be implemented in higher storey space frame building. Suitable MR dampers can be placed to the structure and the responses can be studied.

APPENDIX I. NOTATION

The following symbols are used in this paper:

a_0 and a_1 = Rayleigh damping coefficients and have units of s^{-1} and s.

$a(g)$ and $b(g)$ are polynomials with respect to the backshift operator g^{-1}.

$[A(.)]$ = state (or system) matrix; $\dim[A(.)] = n \times n$

$[B(.)]$ = input matrix; $\dim[B(.)] = n \times r$;

$[C(.)]$ = output matrix; $\dim[C(.)] = q \times n$

$\Gamma = [1 \quad 0 \quad 0]^T$ = the position vector for MR damper force in the structural frame

$\Lambda = [1 \quad 1 \quad 1]^T$ = the position vector for earthquake force on the structural frame

$[D(.)]$= feed-forward matrix; $\dim[D(.)] = q \times r$

E_d = the expected value

f = measured control input force provided by MR damper; F is the control input force vector required in LQG design

$f_g(t)$ = dynamic load with time t.

J = quadratic cost function of Linear Gaussian control;
K= feedback matrix for stabilizability criteria.
$K_a(t)$ = Kalman gain for LQG design
$K_c(s)$ = the feedback controller
L = a Laplace Transform
$L_a(t)$= feedback gain for LQG design
$Maxit$= Maximum iteration for PSO algorithm
$o(h)$ is the system outputs.
O = the observability matrix.
$P(t)$ = solution of Ricatti that solves Linear quadratic estimation problem (LQE)
$Q(t)$ and $R(t)$ = weighting matrices
r_1 and r_2 = random numbers independent of each other between [0,1];
S_r = state controllability matrix
$S(t)$= Ricatti equation that solves Linear quadratic regulator problem
T = final time (horizon);
T_o = output controllability matrix
$u = [u_1 + u_2 + u_3]'$ is a vector of the displacements of the three floors relative to the ground.
u_d is the vertical displacement of the TLCD liquid.
$V_m(t)$ and $W(t)$ = noise intensity matrices
v_m= measurement noise vector
W_i= domain of set of particles i.e. $e_i = (e_{i1}, e_{i2}, e_{i3} \ldots\ldots\ldots, e_{iS})$
$\ddot{x}_g$= a one-dimensional ground acceleration
x = input (or control) vector; $\dim[x(.)] = r \times 1$
$y(.)$ = output vector; $\dim[y(.)] = q \times 1$
$z(.)$ = the state vector; $\dim[z(.)] = n \times 1$

Disclosures

Free Access to this article is sponsored by SARL ALPHA CRISTO INDUSTRIAL.

REFERENCES

1. Fisco NR, Adeli H. Smart structures: Part I—Active and semi-active control. *Sci. Iran.* 2011;275-284.
2. Kerboua M, Benguedia M, Megnounif A, Benrahou KH, Kaoulala F. Semi Active Control of Civil Structures, Analytical and Numerical Studies. *Phy. Proc.* 2014;55:301-306.
3. Spencer BF, Dyke SJ, Sain MK, Carlson JD. Phenomenological model for magnetorheological dampers. *J. Eng. Mec. ASCE*. 1997;123(3):230-238.
4. Yoshioka H, Ramallo JC, Spencer BF. Smart base isolation strategies employing magnetorheological dampers. *J. Eng. Mech. ASCE.* 2002; 128(5):540-551.
5. Xia PQ. An inverse model of MR damper using optimal neural network and system identification. *JSV* Elsevier. 2003;266(5):1009-1023.
6. Khan SA, Suresh A, Ramaiah NS. Principles, characteristics and applications of magneto rheological fluid damper in flow and shear mode. *Procedia Materials Science, Elsevier*. 2014; 6: 1547-1556.
7. Park JM, Gang HG, Sohn JW. Parametric study on damping force characteristics of MR damper with various inner magnetic core shapes. *ICSV2.* 2015;1-2.
8. Cha YJ, Zhang J, Dong B, Friedman A, Agrawal AK, Dyke SJ, Ricles J. Comparative studies of semi-active control strategies for MR dampers. *J. Chem. Inf. Model.* 2013;53(212):1689–1699.
9. Jansen LM, Dyke SJ. Semiactive control strategies for MR dampers : comparative study. *J. Eng. Mech. ASCE*. 2000;126:795–803.
10. Kwok NM, Ha QP, Samali B. MR damper optimal placement for semi-active control of buildings using an efficient multi - objective binary genetic algorithm. *ISARC, I.I.T Madras.* 2007;361-367.
11. Uz M, Hadi MN. SOptimal design of semi active control for adjacent buildings connected by MR damper based on integrated fuzzy logic and multi-objective genetic algorithm. *Engg. Struct. Elsevier.* 2014;69:135–148.
12. Aly AM. Vibration control of buildings using magnetorheological damper : a new control algorithm. *J. Eng. Hindawi.* 2013;*1-10.*
13. Kim HS. Seismic response reduction of a building using top-story isolation system with MR damper. *Contemp. Eng. Sci.* 2014;7(21):979–986.
14. Chang CM, Wang Z, Spencer BF, Chen Z. Semi-active damped outriggers for seismic protection of high-rise buildings. *Smart Structures and Systems*. 2013;11(5):435–451.
15. Bathei A, Zahrai SM, Ramezani M. Semi-active seismic control of an 11-DOF building model with TMD +MR damper using type 1 and type 2 fuzzy algorithms. *JSV SAGE*. 2017;1(16).
16. Hu Y, Liu L, Rahimi S. Seismic vibration control of 3D steel frame with irregular plans using eccentrically placed MR dampers. *Sustainability.* 2017; 9(7):1-20.
17. Gendeshmin SR, Davarnia D. Using block pulse function for seismic vibration semi-active control of structures with MR dampers. *Results in Physics Elsevier*. 2018;8:914-919.
18. Wang J, Sano A, Chen T, Huang B. Identification of Hammerstein systems without explicit parameterisation of non-linearity. *Int. J. Control*. 2009;82:937-952.
19. Chopra A. *Dynamics of Structures Theory and Application to Earthquake Engineering.* USA: Prentice Hall; 2012.
20. Kuo B. Automatic control systems. USA: Prentice Hall; 1975.
21. Ogata K. *Modern Control Engineering.* USA: Prentice

Hall; 2010.

22. Rahmat FM, Ling GT, Hussain AR, Jusoff K. Accuracy comparison of ARX and ANFIS model of an electro-hydraulic actuator system. *Int. J. Smart Sensing Intell. Syst.* 2011;4(3):440-453.

23. Den Hartog JP. *Mechanical Vibrations*. USA: McGraw-Hill; 1956.

24. Gur S, Roy K, Mishra SK. Tuned liquid column ball damper for seismic vibration control. *Struct. Control Health Monit*. 2015;22:1325-1342.

25. Murudi M, Banerji P. Effective control of earthquake response using tuned liquid dampers. *ISET J. Earthq. Tech.* 2010;49(3-4):53-71.

26. Bidgeli Y, Kim D. Response control of irregular structures using structure-TLCD coupled system under seismic excitations. KSCE J. Civil Engg. 2015;19(3):672-681.

27. Farshidianfar A, Soheili S. Optimized tuned liquid column dampers for earthquake oscillations of high-rise structures including soil effects. *Int. J. Optim. Civil Eng.* 2012; 2(2):221-234.

28. Hochrainer MJ. Tuned liquid column damper for structural control. Acta Mechanica. 2005;175:57-76.

29. Kenny A, Broderick B, McCrum DP. Optimisation of a tuned liquid column damper for building structures. 11th Int Conf. RASD. 2013.

30. Dyke SJ, Spencer BF, Sain MK, Carlson JD. Modeling and control of magnetorheological dampers for seismic response reduction. *Smart Mater. Struct.* 1996;5(5):565–575.

31. Lee KS, Fan CP, Sauce R, Ricles J. Simplified design procedure for frame buildings with viscoelastic or elastomeric structural dampers. *Earthquake Eng. Struct. Dynam.* 2005;34(10):1271-1284.

32. Dyke SJ, Spencer BF, Sain MK, Carlson JD. An experimental study of MR dampers for seismic protection. *Smart Mater. Struct*. 1998;7:693–703.

33. Akaike H. A new look at the statistical model identification, *IEEE Aut. Contr.* 1974;19:716 – 723.

34. Bozdogan H. Model selection and Akaike's Information Criterion (AIC): The general theory and its analytical extensions. *Springer-Verlag*. 1987;52:345–370.

35. Peng H, Ozaki T, Toyoda,Y, Shioya H, Nakano K,Ozaki VH, Mori M. RBF-ARX model-based nonlinear system modeling and predictive control with application to a NOx decomposition process. *Control Engineering Practice Elsevier.* 2004;12:191–203.

36. Pant M, Thangaraj R, Abraham A. Particle swarm optimization: performance tuning and empirical analysis. *Foundations*. 2009;3:101–128.

37. Paz M. *Structural dynamics theory and computation.* New York: Thompson Publishing Company; 1991.

38. Chaudhuri, P. and Maity, D. (2020).“Cost optimization of rectangular RC footing usingGA and UPSO.” *Soft Computing,* 24 (January), 709–721.

39. Barman, S. K., Jebieshia, T. R., Tiwari, P, Maiti, D.K. and Maity, D. (2019) “Two-StageInverse Method to Detect Delamination in Composite Beam Using VibrationResponses” *AIAA Journal.* 57 (3). 1312-1322.

40. Barman S.K., Maiti D.K., Maity D. (2020a) Damage Detection of Truss EmployingSwarm-Based Optimization Techniques: A Comparison. In: Venkata Rao R., TalerJ. (eds) Advanced Engineering Optimization Through Intelligent Techniques.Advances in Intelligent Systems and Computing, 949. 21-37 Springer, Singapore.

41. Barman S.K., Maiti D.K., Maity D. (2020b) A New Hybrid Unified Particle Swarm Optimization Technique for Damage Assessment from Changes of Vibration Responses. In: Singh B., Roy A., Maiti D. (eds) Recent Advances in Theoretical, Applied, Computational and Experimental Mechanics. Lecture Notes in Mechanical Engineering. 277-295, Springer, Singapore